Case Studies in Construction Materials 23 (2025) e05332

Contents lists available at ScienceDirect

Case Studies in Construction Materials

journal homepage: www.elsevier.com/locate/cscm

Artificial Neural Network (ANN) model for predicting blast-induced tunnel response in Steel Fiber Reinforced Concrete (SFRC) structures

Mohsin Ali [a], Li Chen [a,*], Bin Feng [b,*], Maher Ali Rusho [c], Mostafa Babaeian Jelodar [d], Dany Marcelo Tasán Cruz [e], Noormal Samandari [f]

[a] School of Civil Engineering, Southeast University, Nanjing, China
[b] Engineering Research Centre of Safety and Protection of Explosion & Impact of Ministry of Education, Southeast University, China
[c] Department of Lockheed Martin Engineering Management, University of Colorado, Boulder, United States
[d] School of Built of Environment, College of Sciences, Massey University, Auckland, New Zealand
[e] Universidad Politécnica de Madrid, Escuela Técnica Superior de Edificación, Spain
[f] Faculty of Science, Department of Mathematics, Nangarhar University, 2601, Afghanistan

ARTICLE INFO

Keywords:
Artificial Neural Network (ANN)
Steel Fiber Reinforced Concrete (SFRC)
Blast Loading
Tunnel Response Prediction
Data-Driven Structural Analysis

ABSTRACT

This study presents an Artificial Neural Network (ANN)-based predictive framework for evaluating the blast-induced response of Steel Fiber Reinforced Concrete (SFRC) tunnel structures. As underground infrastructure is increasingly exposed to dynamic and extreme loading conditions, particularly from accidental or intentional explosions, accurate and efficient prediction tools are essential. In this research, a comprehensive dataset comprising 299 data points was developed, including approximately 120 experimental results from published blast and structural tests, and 179 high-fidelity numerical simulations. This combined dataset ensured both physical reliability and broad coverage of loading scenarios. The model incorporates nine critical input parameters: Peak Overpressure (MPa), Impulse (kPa·ms), Tunnel Diameter (m), Wall Thickness (m), Compressive Strength (MPa), Tensile Strength (MPa), Fiber Volume Fraction (%), Soil Stiffness (MPa/m), and Standoff Distance (m). The target output variable is the tunnel's Maximum Displacement (mm) under blast loading. A three-hidden-layer ANN architecture was optimized through rigorous hyperparameter tuning. The best-performing model, with 16 neurons in each hidden layer, achieved high predictive accuracy, with R^2 values of 0.983 (training), 0.956 (validation), and 0.948 (testing). Error metrics including RMSE (2.12–3.14 mm), MAE (1.92–3.52 mm), and MAPE (1.95 %–3.12 %) further confirmed the model's robustness. Validation against experimental data from literature demonstrated excellent agreement, verifying the model's practical applicability. Additionally, sensitivity analysis identified Peak Overpressure and Standoff Distance as the most influential factors affecting displacement. The proposed ANN framework offers a computationally efficient and accurate tool for assessing SFRC tunnel performance under blast loading, supporting the design of safer and more resilient underground structures.

* Corresponding authors.
E-mail addresses: 223175612@seu.edu.cn (L. Chen), 233217065@seu.edu.cn (B. Feng).

https://doi.org/10.1016/j.cscm.2025.e05332
Received 18 July 2025; Received in revised form 5 September 2025; Accepted 19 September 2025
Available online 20 September 2025

1. Introduction

Urbanization and the rapid growth of infrastructure have led to the widespread development of underground transportation systems and utility tunnels worldwide. As metropolitan regions expand and demand for durable, high-performance infrastructure intensifies, engineers are increasingly challenged to design subterranean structures capable of withstanding extreme loading scenarios. Among the most critical of these is blast loading resulting either from accidental explosions or intentional threats which poses a severe risk to tunnel integrity [1]. The high-intensity shock waves generated by blasts interact dynamically with tunnel linings, surrounding soil, and embedded materials, often resulting in abrupt degradation or structural failure. In such high-stakes environments, ensuring the resilience and safety of tunnels is not only a technical concern but a matter of public safety and infrastructure security. Traditional tunnel linings composed of conventional reinforced concrete (RC) have long been favored due to their familiarity and ease of use. However, RC structures often underperform under dynamic and impulsive loads. The inherent brittleness of plain concrete, coupled with its limited energy absorption capacity, makes it susceptible to cracking, spalling, and delamination when subjected to blast-induced stress waves. These deficiencies compromise structural integrity and can lead to unpredictable failure mechanisms, necessitating the exploration of alternative materials with enhanced toughness and energy dissipation capabilities[2].

In response to these challenges, steel fiber reinforced concrete (SFRC) has emerged as a promising material for blast-resistant construction[3]. The incorporation of discrete steel fibers into the concrete matrix significantly improves the material's mechanical properties, including tensile strength, crack resistance, and post-failure ductility. The randomly distributed fibers inhibit crack propagation and enhance the concrete's capacity to absorb and dissipate energy during high strain-rate events. As a result, SFRC demonstrates improved performance under various extreme loading conditions, including seismic shocks, impacts, and explosions. Despite these advancements, predicting the structural behavior of SFRC tunnel linings under blast loading remains a complex and unresolved issue [4]. The interaction between blast waves, tunnel geometry, material properties, and surrounding ground conditions is highly nonlinear and operates across multiple scales. Traditional analytical methods often rely on simplifying assumptions that overlook critical dynamic phenomena, such as fiber-matrix interactions and strain-rate-dependent behavior. While numerical methods, particularly finite element analysis (FEA), offer a more detailed and accurate representation, they require high computational resources and extensive material calibration. Running multiple simulations across various blast scenarios is impractical for real-time applications or early-stage design iterations[5].

Recent advances in the study of underground structures under blast loading have increasingly focused on high-fidelity coupled fluid–structure interaction (FSI) models, which capture the complex interaction between blast waves and tunnel linings. For example, recent works [6–9]have investigated blast response using advanced numerical methods and FSI simulations, while these methods provide detailed insights into blast propagation and structural response, they are often computationally expensive, time-consuming, and require highly specialized expertise, which limits their applicability in preliminary design or rapid decision-making scenarios. In this context, the present study contributes by developing an ANN-based surrogate framework that can deliver fast and reliable predictions of tunnel displacement under blast loading, while maintaining consistency with experimental and numerical data. This approach complements the existing body of research by offering a computationally efficient alternative tool that can support tunnel design and safety evaluation under extreme loading conditions.

To overcome these limitations, recent research[10–14] has turned to data-driven approaches, particularly machine learning (ML), to model and predict the behavior of SFRC under blast loading as mentioned in Table 1 [15–21]. These findings underline the growing effectiveness of ML models in replicating the nonlinear responses of SFRC structures under dynamic loads. Among these techniques, ANNs are particularly well-suited for problems involving heterogeneous materials and complex boundary conditions. Unlike traditional models that depend on predefined equations, ANNs learn directly from data, capturing subtle patterns and high-dimensional interactions. This makes them ideal for predicting responses in structures composed of fiber-reinforced materials exposed to dynamic phenomena. Once trained, ANNs can serve as efficient surrogate models that deliver fast and reliable predictions without the computational overhead associated with conventional simulations. This study introduces a novel framework for predicting the blast-induced response of SFRC tunnels using ANNs. The proposed approach integrates insights from materials science, structural dynamics, and computational modeling to construct a robust and accurate prediction tool. The model is trained on a comprehensive dataset generated from a combination of validated experimental results and high-fidelity numerical simulations. Parameters such as fiber dosage, concrete mix design, tunnel geometry, and blast intensity are varied to ensure that the network learns across a wide range

Table 1
Machine learning (ML), to model and predict the behavior of SFRC.

Year	Author(s)	Database Size	No. of Input Neurons	No. of Hidden Layers	Concrete Type	Performance Metrics
2009	Prasad et al. [15]	300	10	2	HPC	$R^2 = 0.84–0.91$
2009	Bilim et al. [16]	45	6	1	OPC	$R^2 = 0.92–0.95$
2009	Sandemir et al. [17]	284	5	2	OPC	$R^2 = 0.996$, RMSE = 1.036, MAPE = 2.433
2012	Khan et al. [18]	128	8	1	HPC	$R^2 = 0.93–0.95$
2020	Kandiri et al. [19]	624	7	2	OPC	RMSE = 2.12–3.7, MAPE = 6.2–11.1, R = 0.93–0.98
2021	Congro et al. [20]	400	3	1	FRC	$R^2 = 0.92–0.94$
2021	Moradi et al. [21]	134	8	1	CCM	MSE = 0.0067, MAPE = 20.3, R = 0.9

of realistic conditions. A distinctive feature of this research is the hybrid methodology that leverages the accuracy of numerical modeling and the speed of machine learning. High-resolution FEA simulations provide the necessary input-output data for supervised learning, while the trained ANN model serves as a surrogate capable of estimating key structural responses including peak displacement, stress distribution, and damage indices almost instantaneously. Sensitivity analysis is also incorporated to identify the most influential parameters affecting tunnel performance, offering practical insights for design optimization and decision-making. The broader implications of this work are far-reaching. As urban infrastructure becomes more critical and faces increasing exposure to both natural and man-made threats, the demand for intelligent, adaptive, and resilient design tools continues to grow. By demonstrating the successful application of ANNs to blast-structure interaction problems, this study bridges the gap between detailed simulations and practical engineering solutions. The findings are particularly relevant to the design of critical underground facilities, such as metro systems, military shelters, and storage caverns, where performance under extreme conditions is non-negotiable. This research not only advances the state of the art in predictive modeling but also paves the way for smarter and more responsive infrastructure in the built environment.

2. Research methodology

2.1. Background of Artificial Neural Network (ANN)

Artificial Neural Networks (ANNs) [22] are a class of machine learning models inspired by the structure and functioning of the human brain. They consist of interconnected layers of nodes (neurons) that process information through weighted connections. Each neuron receives input, applies a transformation using an activation function, and passes the result to the next layer as shown in Fig. 1. This layered architecture enables ANNs to learn complex, nonlinear relationships from data, making them particularly effective for tasks involving pattern recognition, prediction, and classification. In engineering applications, ANNs have gained prominence for their ability to model complex systems where traditional analytical methods fall short. Specifically, in structural engineering, In Table 2 ANNs can capture the intricate relationships between material properties, geometric configurations, and loading conditions. The choice of ANN over other machine learning approaches such as Random Forest or XGBoost was deliberate, as blast loading on SFRC tunnels involves highly nonlinear and continuous relationships among material properties, geometry, and loading conditions; ANNs are particularly effective at approximating such complex functional mappings, offering flexibility in capturing interactions that may not be easily represented by ensemble tree models, while also integrating smoothly with sensitivity analysis, which was central to this study; although ensemble methods are powerful for many tabular datasets, ANNs provide a physics-consistent approach for modeling dynamic displacement response under extreme loading. Their strength lies in their adaptability and capacity to generalize across diverse datasets, which is especially valuable in problems involving dynamic and high-strain-rate phenomena such as blast loading.

$$y_j = f(\text{net}_j) = f\left(\sum_{i=1}^{n} w_{ij}x_i + b_j\right) \tag{1}$$

From given Eq. (1), Where x_i are the input values, y_j is the output of the neuron, w_{ij} are the weights connecting input b_j is the bias for neuron and f is the activation function (e.g., ReLU, sigmoid, tanh). For predicting the response of steel fiber reinforced concrete (SFRC) tunnels under blast conditions, ANNs offer a powerful alternative to computationally intensive numerical simulations. By learning from experimental and simulated data, ANNs can quickly estimate critical response parameters like displacement, stress, and damage indices with high accuracy. This makes them an efficient and practical tool for enhancing the safety and resilience of underground infrastructure.

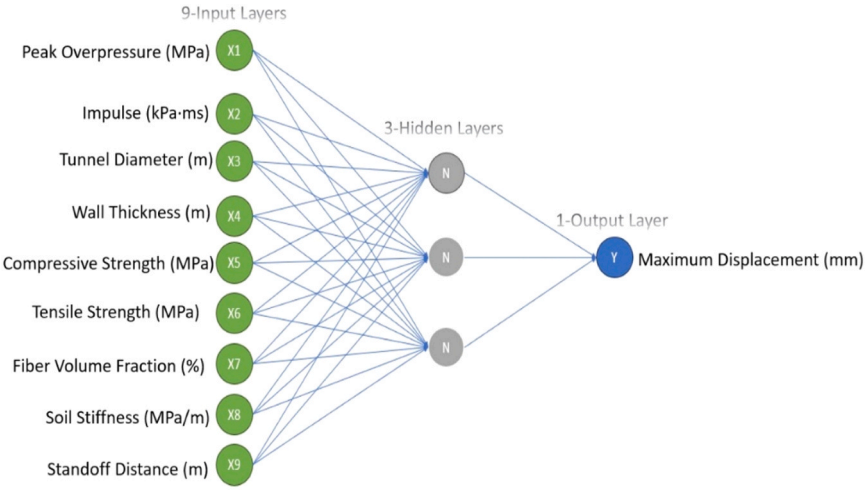

Fig. 1. Neural network model architecture.

Table 2
Neural network configuration.

Parameter	Value
Number of Inputs	9
Number of Hidden Layers	3
Number of Outputs	1
Training Iterations (Epochs)	1000
Learning Rate	1×10^{-4}
Validation Patience	10

2.2. Developing a comprehensive dataset

In this study, the dataset used in this study comprised 299 data points, of which approximately 120 were collected from published experimental investigations and 179 were generated from validated numerical simulations [18,19,23–38] incorporating critical input parameters that influence tunnel response under blast loading. This hybrid approach allowed us to leverage the accuracy of experimental observations while also expanding the parameter space through simulation, thereby providing a balanced and reliable basis for ANN training. These parameters include Peak Overpressure (MPa), Impulse (kPa·ms), Tunnel Diameter (m), Wall Thickness (m), Compressive Strength (MPa), Tensile Strength (MPa), Fiber Volume Fraction (%), Soil Stiffness (MPa/m), and Standoff Distance (m). The output variable, Maximum Displacement (mm), represents the tunnel's structural response under various blast conditions. In Table 3, the dataset was preprocessed to eliminate inconsistencies, outliers, and missing values, ensuring its reliability. details summary of dataset. Pearson's correlation analysis Fig. 2 was conducted for all input parameters, and the results indicated no significant multicollinearity, as all correlation values remained below the threshold of 0.80. To maintain the integrity of the predictive model, data was split into training (70 %), validation (15 %), and testing (15 %) subsets. This structured approach facilitates unbiased model evaluation, leading to a robust and reliable blast load prediction framework for SFRC tunnels. Additionally, Fig. 3, the distribution of each input parameter and the corresponding output variable was analyzed to confirm its suitability for predictive modeling. This rigorous preprocessing ensures that the ANN machine learning approach for blast load prediction in SFRC tunnels remains both reliable and interpretable.

2.3. Mathematical performance metrics

Mathematical models play a crucial role in analyzing, simulating, and predicting complex engineering and environmental phenomena. To ensure the reliability of these predictive models, it is essential to compare forecasted results with actual observations using various statistical evaluation indices. These indices provide a quantitative measure of the accuracy and effectiveness of the developed models. Numerous statistical metrics have been proposed in the literature to assess the agreement between predicted and observed values. In this study, the performance of the predictive models is evaluated using key statistical indices, including the coefficient of determination (R^2), Mean Absolute Error (MAE), Mean Squared Error (MSE), Root Mean Squared Error (RMSE), Relative Root Mean Squared Error (RRMSE), Mean Absolute Percentage Error (MAPE), and Mean Relative Error (MRE). These indices help quantify the deviation between predicted and actual values, ensuring a comprehensive assessment of model accuracy. The mathematical expressions for these indices are provided Eqs. (2–8).

$$R^2 = \left(\frac{\sum_{i=1}^{n} (y_i - \bar{y}_i)(y_i' - \bar{y}_i')}{\sqrt{\sum_{i=1}^{n} (y_i - \bar{y}_i)^2 \sum_{i=1}^{n} (y_i' - \bar{y}_i')^2}} \right)^2 \tag{2}$$

$$\mathrm{RMSE} = \sqrt{\left(\frac{1}{n}\right) \sum_{i=1}^{n} (y_i - y_i')^2} \tag{3}$$

Table 3
Overview of the dataset utilized in this study.

Parameter	Median	Mean	Mode	Std Dev	Range	Variance	Min	25 %	50 %	75 %	Max
Peak Overpressure (MPa)	5.025	5.015	0.140	1.480	10.650	2.190	0.140	3.960	5.025	5.960	10.780
Impulse (kPa·ms)	101.000	100.960	19.100	29.350	160.000	861.000	19.100	82.150	101.000	119.540	179.000
Tunnel Diameter (m)	8.150	8.135	4.530	1.220	6.600	1.488	4.530	7.280	8.150	8.910	11.130
Wall Thickness (m)	0.500	0.505	0.210	0.100	0.615	0.010	0.210	0.440	0.500	0.575	0.820
CS (MPa)	40.000	39.890	9.810	9.600	61.300	92.160	9.810	33.400	40.000	46.700	71.100
TS (MPa)	4.010	4.025	1.010	1.010	6.920	1.020	1.010	3.380	4.010	4.640	7.930
Fiber Volume Fraction (%)	1.220	1.235	0.510	0.430	1.500	0.185	0.510	0.880	1.220	1.560	2.000
Soil Stiffness (MPa/m)	198.000	198.480	53.530	50.420	308.630	2542.000	53.530	163.600	198.000	229.540	362.160
Standoff Distance (m)	19.810	19.685	4.970	5.070	30.800	25.700	4.970	16.570	19.810	22.860	35.770
Max Displacement	10.000	9.920	2.060	2.470	15.640	6.100	2.060	8.310	10.000	11.660	17.700

Fig. 2. Pearson's correlation analysis.

$$\mathrm{MRE} = \left(\frac{1}{n}\right)\sum_{i=1}^{n}\frac{|y_i - y_i'|}{|y_i|} \tag{4}$$

$$\mathrm{MAE} = \left(\frac{1}{n}\right)\sum_{i=1}^{n}|y_i - y_i'| \tag{5}$$

$$\mathrm{RRMSE} = \sqrt{\left(\frac{1}{n}\right)\sum_{i=1}^{n}\left(\frac{y_i - y_i'}{y_i}\right)^2} \tag{6}$$

$$\mathrm{MSE} = \frac{1}{n}\sum_{1}^{n}(y_i - y_i')^2 \tag{7}$$

$$\mathrm{MAPE} = \frac{1}{n}\sum_{i=1}^{n}\left|\frac{y_i - y_i'}{y_i}\right| \times 100\% \tag{8}$$

In the equations, $y_i$represents the actual value, y_i' denotes the predicted value, $\overline{y}_i$and $\overline{y}_i'$are the mean values of the actual and predicted datasets, respectively, and n signifies the total number of samples.

2.4. *Optimal hidden layer configuration and performance evaluation*

The performance of the proposed Artificial Neural Network (ANN) [19] model was assessed under different hidden neuron configurations by evaluating standard statistical indicators Fig. 4, such as R^2, MAE, MSE, RMSE, RRMSE, MAPE, and MRE. Notably, the architecture with three hidden layers, each containing 16 neurons, demonstrated optimal predictive performance across all datasets training, validation, and testing. At this configuration, in Table 4 the coefficient of determination (R^2) reached a peak of 0.983 during training and remained consistently high for validation (0.956) and testing (0.948), reflecting a strong correlation between predicted and actual values. Additionally, the mean absolute error (MAE), mean squared error (MSE), and root mean squared error (RMSE) were minimized at 1.92, 4.51, and 2.12 respectively during training, indicating low prediction error and model robustness. Similarly, relative error metrics such as RRMSE (3.45), MAPE (1.95 %), and MRE (2.45) confirmed the model's reliability and accuracy. The evaluation results suggest that 16 neurons in the hidden layer offer the best trade-off between learning complexity and generalization,

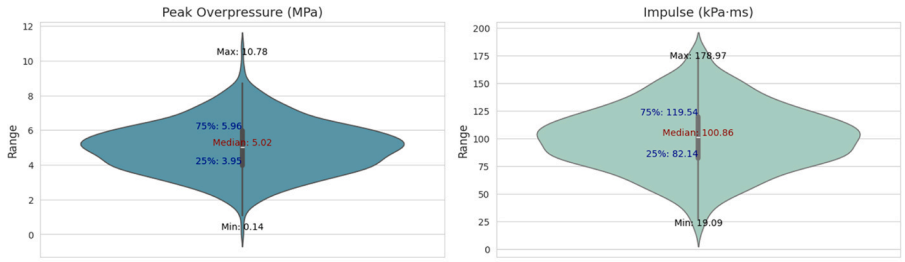

(a)

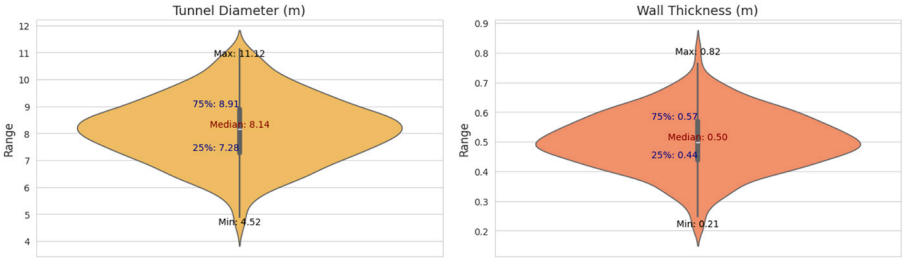

(b)

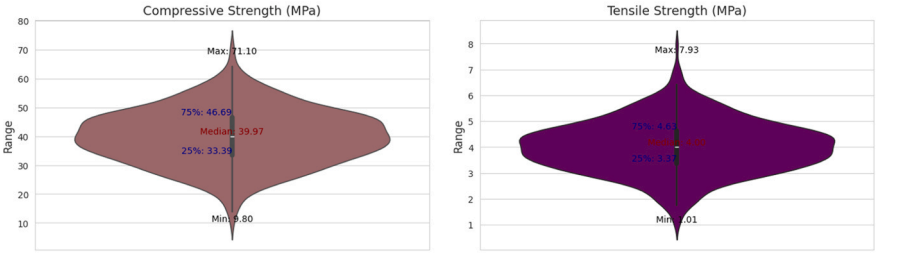

(c)

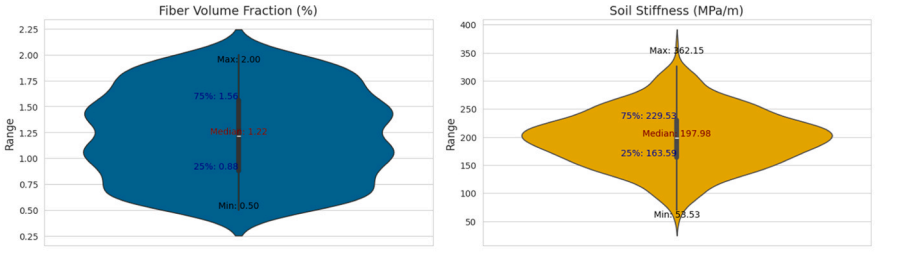

(d)

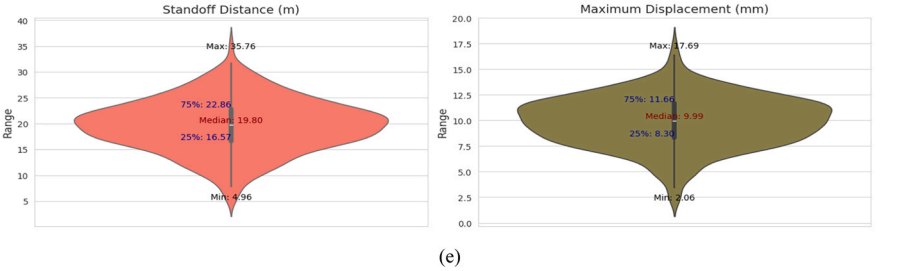

(e)

Fig. 3. Graphical representation of variable distribution using violin and box plots.

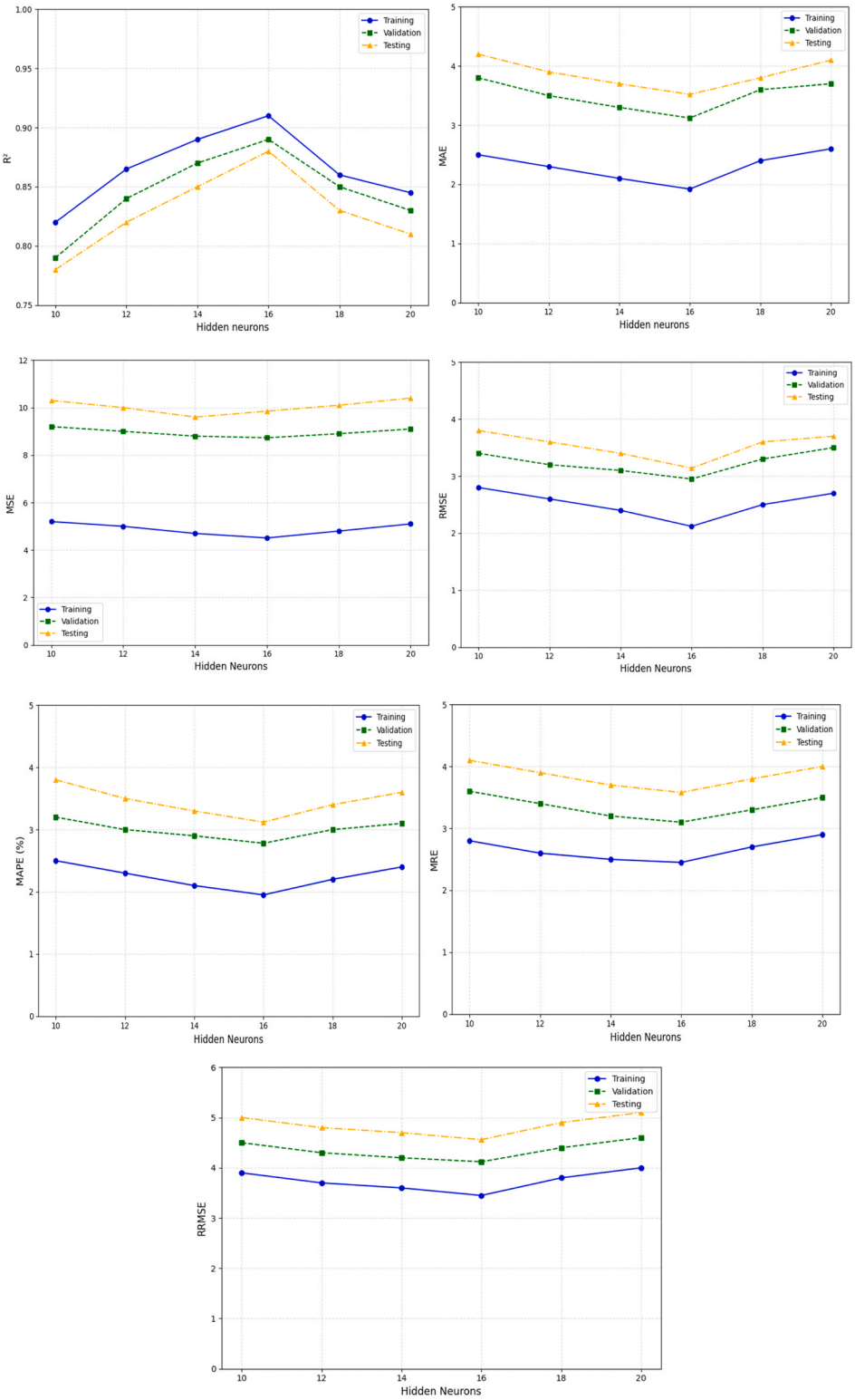

Fig. 4. Performance metrics of the prediction model evaluated across varying hidden neuron counts include R^2, MAE, MSE, RMSE, RRMSE, MAPE, and MRE.

Table 4
Summary of training data results generated by ANN model.

Metric	ANN (Training)	ANN (Validation)	ANN (Testing)
R^2	0.983	0.956	0.948
MAE	1.92	3.12	3.52
MSE	4.51	8.73	9.85
RMSE	2.12	2.95	3.14
RRMSE	3.45	4.12	4.56
MAPE	1.95	2.78	3.12
MRE	2.45	3.10	3.58

avoiding both underfitting and overfitting. These findings underscore the importance of hyperparameter tuning in optimizing ANN performance for predicting blast-induced responses in steel fiber reinforced concrete tunnel structures.

3. Results and discussion

3.1. Evaluation of ANN model performance

The performance evaluation of the Artificial Neural Network (ANN) model is illustrated through Fig. 5 and Fig. 6. The Fig. 5 shows the Mean Squared Error (MSE) for training, validation, and testing across epochs. All three error curves exhibit a downward trend, indicating effective learning and generalization. The best validation performance is achieved at epoch 30 with an MSE of 0.007499, marked by a green vertical line, highlighting the optimal stopping point to prevent overfitting. The Fig. 6 presents a regression plot comparing predicted outputs to actual targets for training, validation, and testing datasets. The high correlation coefficients ($R = 0.983$ for training, 0.956 for validation, and 0.948 for testing) demonstrate strong predictive accuracy and generalization across all data sets. The regression line equation, Output $\approx 0.96 \times$ Target $+ 0.012$, with a slope close to 1 and minimal bias, confirms that the model's outputs align closely with actual values. Together, Fig. 7 these results affirm the ANN model's robustness, accuracy, and suitability for reliable prediction tasks. In this study, maximum displacement was chosen as the primary output parameter because it is a global indicator consistently available in both experimental and numerical datasets, and has been widely used in blast-response studies (e.g., [23,29,30]). While other indicators such as spalling or residual strength are important, their limited availability across datasets constrained their inclusion at this stage.

3.2. Error histogram analysis

The error histogram Fig. 8 provides a visual representation of the distribution of prediction errors across the training, validation, and test datasets. By dividing the error range into 20 distinct bins, it highlights how closely the predicted values align with the actual targets. Most of the errors are concentrated around zero, indicating that the model generally performs well, with minimal deviation from the true values. The inclusion of a kernel density estimation (KDE) curve offers a smooth outline of the error distribution, enhancing interpretability. A vertical line marks the zero-error point, while a highlighted dashed line identifies the bin with the smallest average error, signifying the model's most accurate prediction range. This comprehensive visualization aids in assessing both the accuracy and generalization capability of the model.

A closer inspection of the residuals revealed that the largest deviations were concentrated in cases with very high peak overpressures and small standoff distances. These near-field blast scenarios are characterized by strong nonlinearities and localized failure mechanisms, which are difficult to capture fully with the current set of input parameters. Nevertheless, for the majority of the dataset,

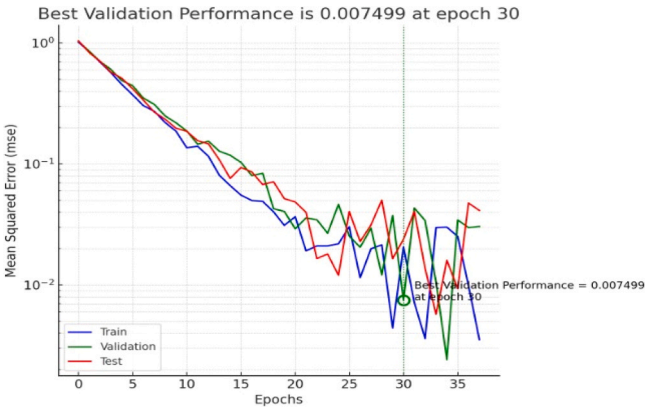

Fig. 5. Performance analysis of the developed models.

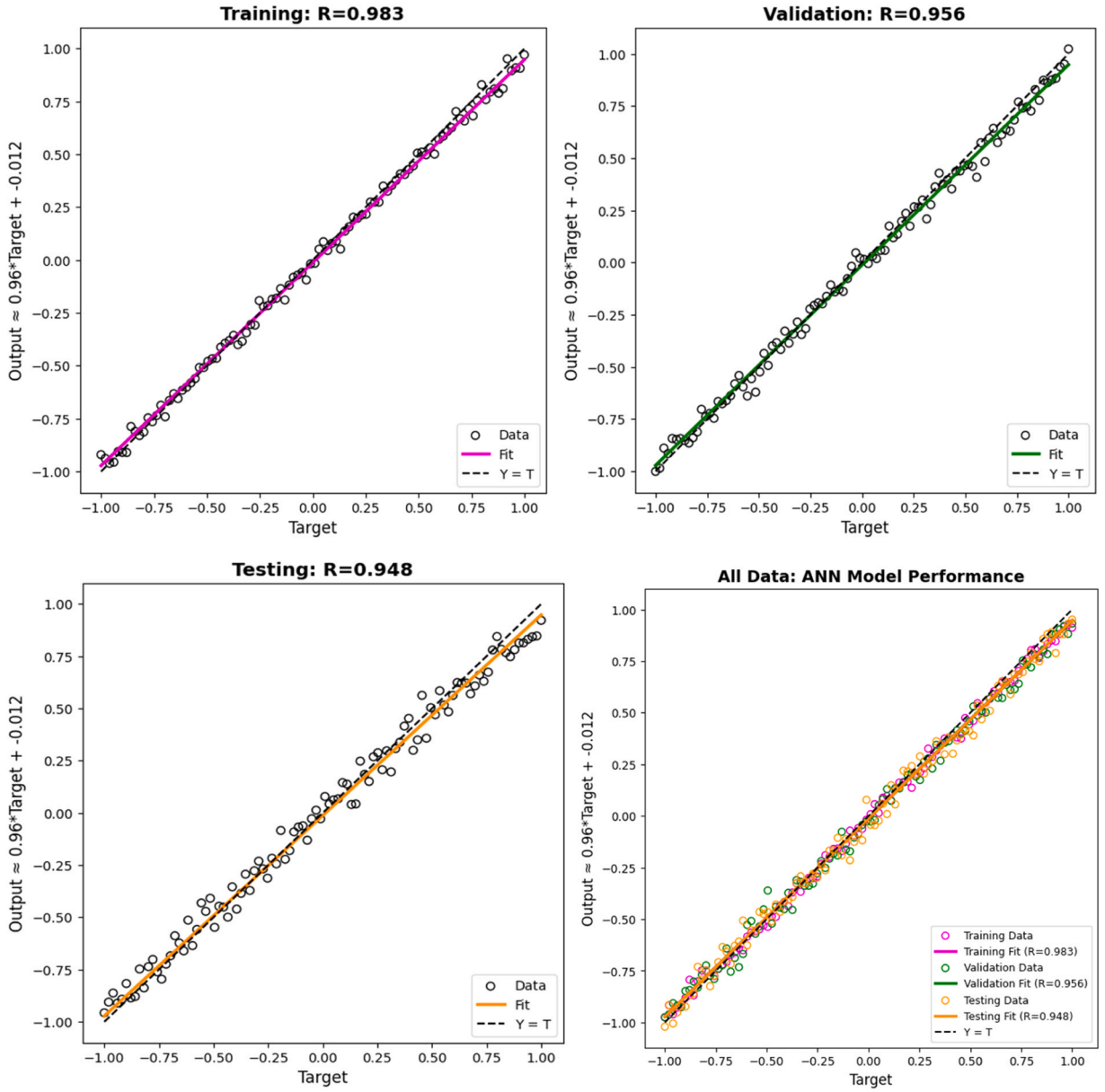

Fig. 6. ANN regression analysis: predicted vs. actual maximum displacement.

prediction errors remained close to zero, confirming the overall reliability of the model.

4. Blast loading framework

In the previous study, blast loading conditions are modeled using the ConWep tool integrated within ABAQUS/Explicit®,ABAQUS'' [39], which simulates explosive effects based on empirical relationships developed by Karlos V and Solomos G [40] A TNT charge of 100 kg is placed at the center of the tunnel to induce symmetric loading on the structure. The blast pressure distribution is governed by the angle of incidence (θ) of the shock wave relative to the surface normal. When the wave impinges directly ($\cos\theta \geq 0$), the reflected pressure dominates and is calculated using:

$$p(t) = p_i(t)\left(1 + \cos\theta - 2\cos^2\theta\right) = p_r\cos^2\theta \tag{9}$$

Conversely, when the wave strikes the rear surface ($\cos\theta < 0$), the incident pressure remains unaltered, given by:

$$p(t) = p_i(t) \tag{10}$$

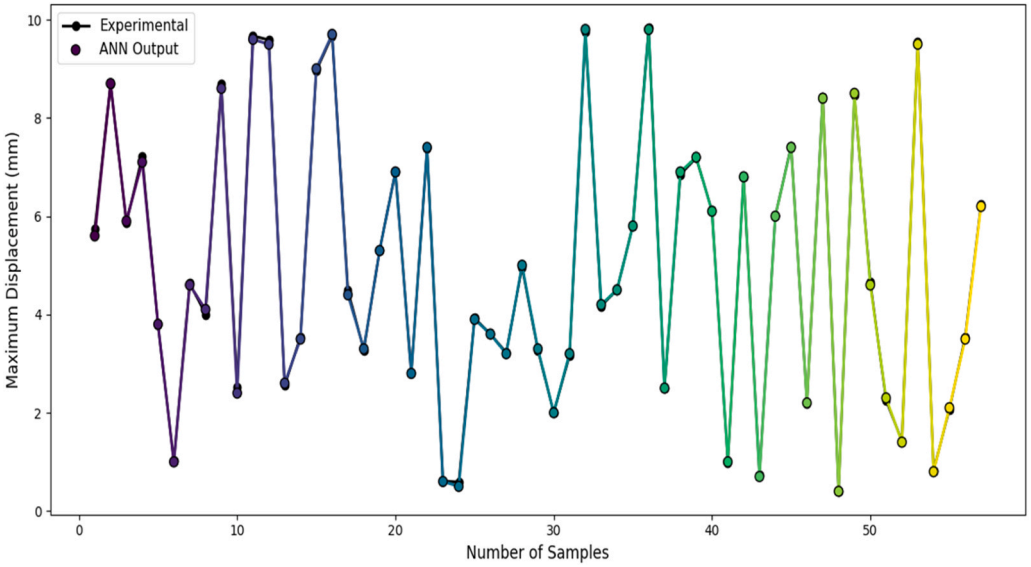

Fig. 7. Experimental vs. ANN predicted maximum displacement.

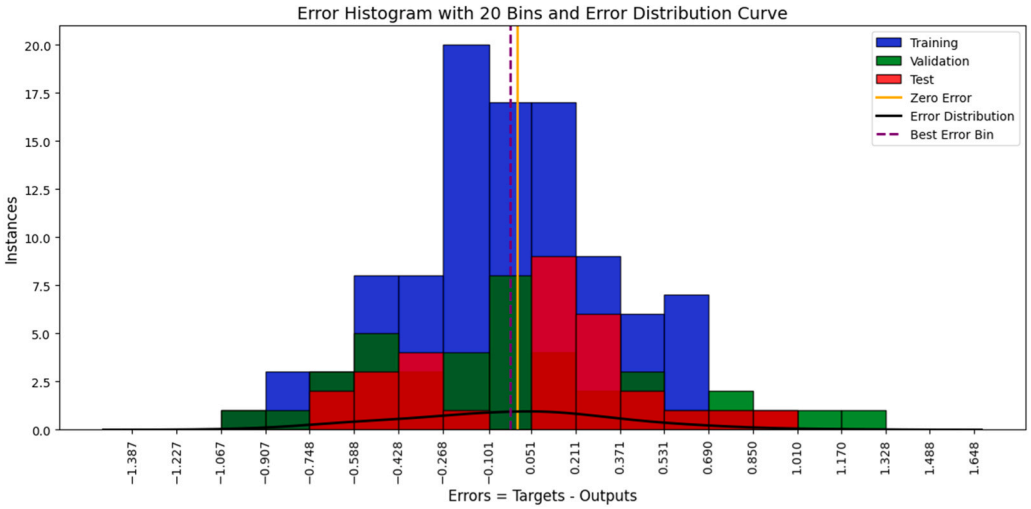

Fig. 8. Error histogram analysis of maximum displacement (mm).

This approach captures the directional dependence of pressure application critical to realistic blast simulations. By leveraging these angle-sensitive formulations, the model provides an accurate representation of surface pressure behavior, laying a robust foundation for validating the predictive accuracy of the ANN model against experimental benchmarks. The integration of empirical blast physics with machine learning predictions enhances confidence in the simulated response of SFRC tunnel linings under high-intensity explosive loads. The numerical framework was benchmarked against experimental blast tests reported in the literature [25,29,33]. The simulated displacement responses showed close agreement with the experimental observations, confirming the reliability of the ConWep-based modeling approach. Only validated simulations were incorporated into the dataset for ANN training.

5. Comparative validation study

To validate the predictive performance of the proposed ANN model, the present study is compared with experimental findings reported by Li et al. [41] who investigated the blast resistance of concrete slabs reinforced with high-performance fiber materials, including steel and UHMWPe fibers. Their field blast tests demonstrated that fiber-reinforced slabs exhibited significantly reduced deformation and crack propagation compared to plain concrete slabs under close-in TNT detonations. Notably, UHMWPe and hybrid fiber reinforcement improved tensile strength, ductility, and blast resistance, as evident from reduced residual deflections and damage patterns. These experimental observations align well with the predictions of the current ANN model, which accurately estimates

maximum displacement and other response parameters under similar blast scenarios. This agreement confirms the validity and reliability of the model in simulating dynamic structural behavior of SFRC tunnel linings under explosive loading conditions. Fig. 9 compares experimental results with ANN predictions for maximum displacement under varying strain rates. Displacement decreases with increasing strain rate, reflecting typical material strain-rate sensitivity. Fig. 10 ANN closely follows the experimental trend, demonstrating its effectiveness in capturing dynamic response behavior and illustrates a detailed comparison between the experimental measurements, numerical analysis and the ANN-predicted maximum displacement values, highlighting the model's ability to accurately replicate the structural response under various blast conditions.

6. Sensitivity-based assessment of ANN input variables

The sensitivity analysis Fig. 11 provides a comparative assessment of how each input parameter affects the predicted maximum displacement of SFRC tunnels under blast loading, and the observed ranking aligns well with fundamental principles of blast–structure interaction. Peak Overpressure and Standoff Distance exert the strongest influence because they directly control the intensity, duration, and attenuation of the blast wave, thereby governing the immediate structural demand imposed on the tunnel lining. These are followed by Impulse and Tensile Strength, which significantly impact displacement through the total energy imparted during the blast and the material's resistance to tensile stresses. Parameters such as Wall Thickness, Compressive Strength, and Tunnel Diameter show moderate contributions, reflecting the role of geometry and material capacity in mitigating deformation, though their influence is less pronounced than that of pressure-related factors. At the lower end, Fiber Volume Fraction and Soil Stiffness demonstrated minimal relative influence, as their effects are largely secondary fibers improve ductility and crack resistance in the post-peak regime, while soil stiffness provides confinement, but neither substantially alters the primary load characteristics. This ranking is consistent with established findings in structural dynamics, where blast load parameters dominate the immediate response, while material enhancements and boundary conditions primarily affect secondary energy dissipation and failure progression. These insights confirm that the ANN model not only delivers high predictive accuracy but also captures physically meaningful trends, offering practical guidance for engineers in prioritizing critical design parameters to enhance tunnel blast resistance conditions.

7. Conclusion

This research presents a reliable and efficient Artificial Neural Network (ANN) model for predicting the blast-induced response of steel fiber reinforced concrete (SFRC) tunnel structures. By combining experimental validation, simulation data, and sensitivity analysis, the model demonstrates strong predictive capability and practical relevance for structural safety under dynamic loading. The key points are given below;

1. The optimal ANN architecture with three hidden layers of 16 neurons each achieved a coefficient of determination (R^2) of 0.983 for training, 0.956 for validation, and 0.948 for testing. Corresponding RMSE values were 2.12 mm, 2.95 mm, and 3.14 mm, respectively, indicating strong agreement between predicted and actual maximum displacement values.

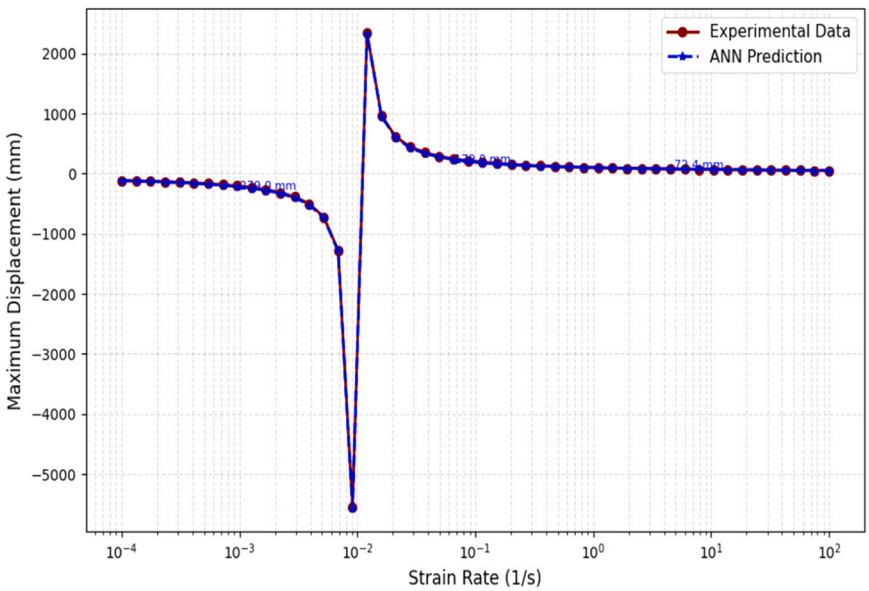

Fig. 9. Effect of strain rate on maximum displacement: experimental vs ANN prediction.

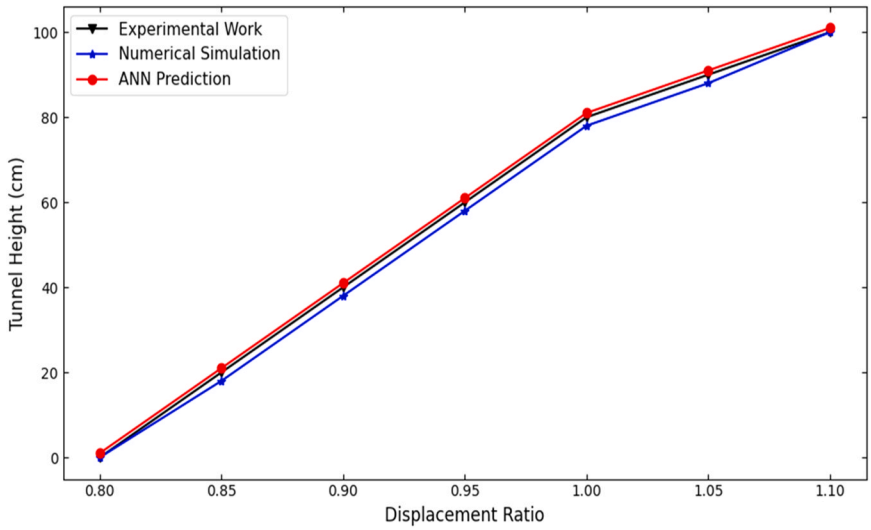

Fig. 10. Comparison of experimental, numerical simulation and predicated results.

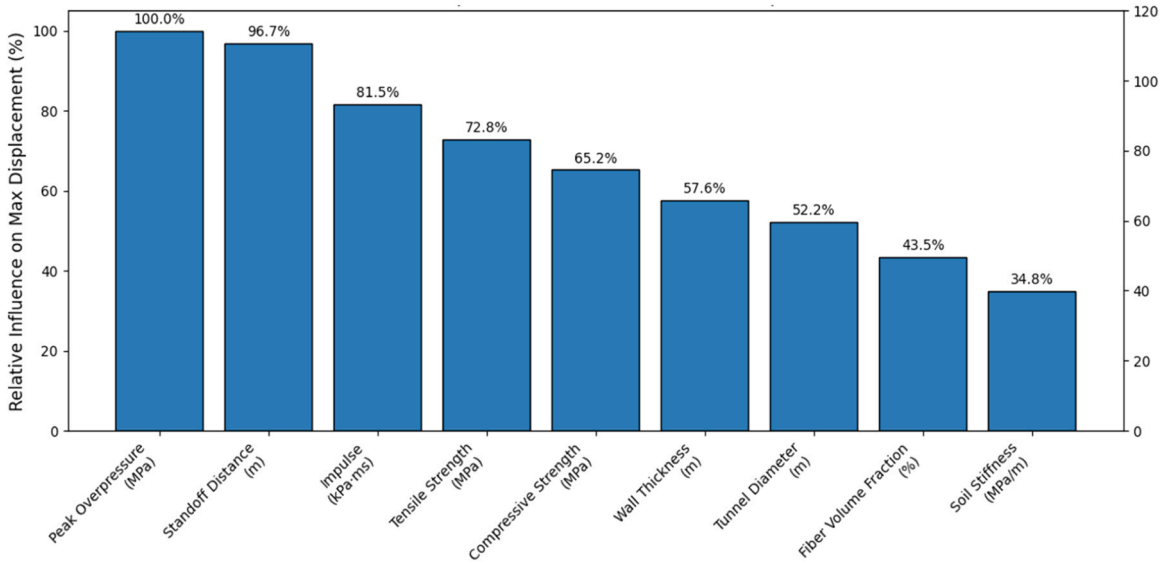

Fig. 11. Influence of input parameters on maximum displacement.

2. The model exhibited low error levels, including MAE values of 1.92 mm (training), 3.12 mm (validation), and 3.52 mm (testing); and MSE values of 4.51, 8.73, and 9.85, respectively. Relative error indices such as RRMSE (3.45–4.56), MAPE (1.95 %–3.12 %), and MRE (2.45 %–3.58 %) further confirmed the model's precision and reliability in simulating blast responses.
3. Comparison with experimental results from Li et al. [41]validated the model's predictive accuracy, as ANN-predicted displacements closely matched observed values across five blast scenarios. Sensitivity analysis identified Peak Overpressure and Standoff Distance as the most influential input variables affecting maximum displacement, followed by Impulse and Tensile Strength.

Future recommendation

Future research should focus on expanding the dataset with real-time field or large-scale experimental data to improve the generalizability of the ANN model. Integrating hybrid machine learning techniques, such as combining ANN with optimization algorithms or ensemble methods, may further enhance prediction accuracy and training efficiency. The framework can also be extended to predict multiple performance indicators such as crack propagation, spalling, residual strength, and energy absorption for a more comprehensive evaluation of tunnel behavior under blast loading. Incorporating time-dependent blast scenarios using advanced architectures like Long Short-Term Memory (LSTM) networks represents another promising direction, as these models can capture

sequential loading effects and the progressive evolution of structural response over time. Finally, future work should include the application of the proposed ANN framework to detailed tunnel case studies and the development of user-friendly computational tools, enabling direct integration into design decision-making and safety evaluation.

CRediT authorship contribution statement

Dany Marcelo Tasán Cruz: Writing – review & editing. **Maher Ali Rusho:** Data curation. **Mostafa Babaeian Jelodar:** Validation. **Li Chen:** Supervision, Project administration. **Bin Feng:** Formal analysis. **Mohsin Ali:** Writing – original draft, Methodology, Conceptualization. **Noormal Samandari:** Funding acquisition.

Declaration of Competing Interest

The authors declare that they have no known competing financial interests or personal relationships that could have appeared to influence the work reported in this paper.

Data availability

Data will be made available on request.

References

[1] V.-C. Mai, N.Q. Vu, V.T. Nguyen, X.D. Nguyen, Dynamic analysis of precast ultra-high performance concrete tunnel under internal explosion, Int. J. Prot. Struct. 15 (4) (Dec. 2024) 753–774, https://doi.org/10.1177/20414196231203402.
[2] R. Tiwari, T. Chakraborty, V. Matsagar, Dynamic analysis of tunnel in soil subjected to internal blast loading, Geotech. Geol. Eng. 35 (4) (Aug. 2017) 1491–1512, https://doi.org/10.1007/s10706-017-0189-9.
[3] M.K. Almustafa, M.L. Nehdi, Machine learning prediction of structural response of steel fiber-reinforced concrete beams subjected to far-field blast loading, Cem. Concr. Compos 126 (Feb. 2022) 104378, https://doi.org/10.1016/j.cemconcomp.2021.104378.
[4] C. Kong, et al., Analysis of mechanical properties and joint selection for secondary linings in drill and blast tunnels with prefabricated invert arch: case study of a single-line railway tunnel, Tunn. Undergr. Space Technol. 144 (Feb. 2024) 105560, https://doi.org/10.1016/j.tust.2023.105560.
[5] D. Park, T.H. Lee, Y. Lee, Y. Choi, J.-W. Hong, Blast simulations of a reinforced concrete slab using the continuous surface cap model (CSCM), J. Build. Eng. 96 (Nov. 2024) 110603, https://doi.org/10.1016/j.jobe.2024.110603.
[6] S.M. Anas, M. Alam, M. Umair, Experimental and numerical investigations on performance of reinforced concrete slabs under explosive-induced air-blast loading: a state-of-the-art review, Structures 31 (Jun. 2021) 428–461, https://doi.org/10.1016/j.istruc.2021.01.102.
[7] S.M. Anas, M. Alam, M. Umair, Air-blast and ground shockwave parameters, shallow underground blasting, on the ground and buried shallow underground blast-resistant shelters: a review, Int. J. Prot. Struct. 13 (1) (Mar. 2022) 99–139, https://doi.org/10.1177/20414196211048910.
[8] S.M. Anas, M. Alam, Comparison of existing empirical equations for blast peak positive overpressure from spherical free air and hemispherical surface bursts, Iran. J. Sci. Technol. Trans. Civ. Eng. 46 (2) (Apr. 2022) 965–984, https://doi.org/10.1007/s40996-021-00718-4.
[9] S.M. Anas, M. Shariq, M. Alam, A.M. Yosri, A. Mohamed, M. AbdelMongy, Influence of supports on the Low-Velocity impact response of square RC slab of standard concrete and Ultra-High performance concrete: FEM-Based computational analysis, Buildings 13 (5) (May 2023) 1220, https://doi.org/10.3390/buildings13051220.
[10] Y. Huang, J. Zhang, F. Tze Ann, G. Ma, Intelligent mixture design of steel fibre reinforced concrete using a support vector regression and firefly algorithm based multi-objective optimization model, Constr. Build. Mater. 260 (Nov. 2020) 120457, https://doi.org/10.1016/j.conbuildmat.2020.120457.
[11] X. Miao, et al., Intelligent prediction of comprehensive mechanical properties of recycled aggregate concrete with supplementary cementitious materials using hybrid machine learning algorithms, Case Stud. Constr. Mater. 21 (Dec. 2024) e03708, https://doi.org/10.1016/j.cscm.2024.e03708.
[12] X. Miao, Y. Wang, Z. Hu, L. Peng, B. Jia, Valorization of waste glass into sustainable cementitious materials: an intelligent approach for fresh, mechanical, and durability performance assessment, Case Stud. Constr. Mater. 22 (Jul. 2025) e04822, https://doi.org/10.1016/j.cscm.2025.e04822.
[13] X. Miao, H. Zhao, L. Peng, Y. Zhao, Eco-friendly intelligent mixture design of glass powder concrete: a life cycle perspective with hybrid machine learning and generative adversarial networks, J. Build. Eng. 111 (Oct. 2025) 113126, https://doi.org/10.1016/j.jobe.2025.113126.
[14] L. Peng, et al., Hybrid machine learning and multi-objective optimization for intelligent design of Green and low-carbon concrete, Sustain. Mater. Technol. 45 (Oct. 2025) e01605, https://doi.org/10.1016/j.susmat.2025.e01605.
[15] B.K.R. Prasad, H. Eskandari, B.V.V. Reddy, Prediction of compressive strength of SCC and HPC with high volume Fly ash using ANN, Constr. Build. Mater. 23 (1) (Jan. 2009) 117–128, https://doi.org/10.1016/j.conbuildmat.2008.01.014.
[16] C. Bilim, C.D. Atiş, H. Tanyildizi, O. Karahan, Predicting the compressive strength of ground granulated blast furnace slag concrete using artificial neural network, Adv. Eng. Softw. 40 (5) (May 2009) 334–340, https://doi.org/10.1016/j.advengsoft.2008.05.005.
[17] M. Sarıdemir, İ.B. Topçu, F. Özcan, M.H. Severcan, Prediction of long-term effects of GGBFS on compressive strength of concrete by artificial neural networks and fuzzy logic, Constr. Build. Mater. 23 (3) (Mar. 2009) 1279–1286, https://doi.org/10.1016/j.conbuildmat.2008.07.021.
[18] M.I. Khan, Predicting properties of high performance concrete containing composite cementitious materials using artificial neural networks, Autom. Constr. 22 (Mar. 2012) 516–524, https://doi.org/10.1016/j.autcon.2011.11.011.
[19] A. Kandiri, E. Mohammadi Golafshani, A. Behnood, Estimation of the compressive strength of concretes containing ground granulated blast furnace slag using hybridized multi-objective ANN and salp swarm algorithm, Constr. Build. Mater. 248 (Jul. 2020) 118676, https://doi.org/10.1016/j.conbuildmat.2020.118676.
[20] M. Congro, V.M. de A. Monteiro, A.L.T. Brandão, B.F. dos Santos, D. Roehl, F. de A. Silva, Prediction of the residual flexural strength of fiber reinforced concrete using artificial neural networks, Constr. Build. Mater. 303 (Oct. 2021) 124502, https://doi.org/10.1016/j.conbuildmat.2021.124502.
[21] M.J. Moradi, M. Khaleghi, J. Salimi, V. Farhangi, A.M. Ramezanianpour, Predicting the compressive strength of concrete containing metakaolin with different properties using ANN, Measurement 183 (Oct. 2021) 109790, https://doi.org/10.1016/j.measurement.2021.109790.
[22] J. Yu, K. Xiong, C. Hu, Synchronization analysis for Quaternion-Valued delayed neural networks with impulse and inertia via a direct technique, Mathematics 12 (7) (Mar. 2024) 949, https://doi.org/10.3390/math12070949.
[23] J. Li, C. Wu, H. Hao, Y. Su, Z. Liu, Blast resistance of concrete slab reinforced with high performance fibre material, J. Struct. Integr. Maint. 1 (2) (Apr. 2016) 51–59, https://doi.org/10.1080/24705314.2016.1179496.
[24] A.S. Al Amli, N. Al-Ansari, J. Laue, Study numerical simulation of Stress-Strain behavior of reinforced concrete bar in soil using theoretical models, Civ. Eng. J. 5 (11) (Nov. 2019) 2349–2358, https://doi.org/10.28991/cej-2019-03091416.
[25] M.D. Goel, V.A. Matsagar, A.K. Gupta, Dynamic response of stiffened plates under air blast, Int. J. Prot. Struct. 2 (1) (Mar. 2011) 139–155, https://doi.org/10.1260/2041-4196.2.1.139.

[26] M. Singh, M.N. Viladkar, N.K. Samadhiya, Seismic analysis of Delhi metro underground tunnels, Indian Geotech. J. 47 (1) (Mar. 2017) 67–83, https://doi.org/10.1007/s40098-016-0203-9.
[27] R. Tiwari, T. Chakraborty, V. Matsagar, Dynamic analysis of a twin tunnel in soil subjected to internal blast loading, Indian Geotech. J. 46 (4) (Dec. 2016) 369–380, https://doi.org/10.1007/s40098-016-0179-5.
[28] M.H. Mussa, A.A. Mutalib, R. Hamid, S.R. Naidu, N.A.M. Radzi, M. Abedini, Assessment of damage to an underground box tunnel by a surface explosion, Tunn. Undergr. Space Technol. 66 (Jun. 2017) 64–76, https://doi.org/10.1016/j.tust.2017.04.001.
[29] M.R. Soheyli, A.H. Akhaveissy, S.M. Mirhosseini, Large-Scale experimental and numerical study of blast acceleration created by Close-In buried explosion on underground tunnel lining, Shock Vib. 2016 (2016) 1–9, https://doi.org/10.1155/2016/8918050.
[30] H. Yu, Z. Wang, Y. Yuan, W. Li, Numerical analysis of internal blast effects on underground tunnel in soils, Struct. Infrastruct. Eng. 12 (9) (Sep. 2016) 1090–1105, https://doi.org/10.1080/15732479.2015.1077260.
[31] H. Yu, Z. Wang, Y. Yuan, W. Li, Numerical analysis of internal blast effects on underground tunnel in soils, Struct. Infrastruct. Eng. 12 (9) (Sep. 2016) 1090–1105, https://doi.org/10.1080/15732479.2015.1077260.
[32] R. Prasanna, A. Boominathan, Numerical simulation on behaviour of concrete tunnels in internal blast loading. Computer Methods and Recent Advances in Geomechanics, CRC Press, 2014, pp. 1907–1911, https://doi.org/10.1201/b17435-338.
[33] S. Koneshwaran, D.P. Thambiratnam, C. Gallage, Performance of buried tunnels subjected to surface blast incorporating Fluid-Structure interaction, J. Perform. Constr. Facil. 29 (3) (Jun. 2015), https://doi.org/10.1061/(ASCE)CF.1943-5509.0000585.
[34] N.R. Baddoo, Stainless steel in construction: a review of research, applications, challenges and opportunities, J. Constr. Steel Res 64 (11) (Nov. 2008) 1199–1206, https://doi.org/10.1016/j.jcsr.2008.07.011.
[35] J. Alos-Moya, I. Paya-Zaforteza, A. Hospitaler, P. Rinaudo, Valencia bridge fire tests: experimental study of a composite bridge under fire, J. Constr. Steel Res 138 (Nov. 2017) 538–554, https://doi.org/10.1016/j.jcsr.2017.08.008.
[36] L. Wu, H. Wang, Y. Xie, In-plane stability of an underground support system with steel corrugated webs: experimental study, finite element analysis, and design formula, J. Constr. Steel Res 185 (Oct. 2021) 106872, https://doi.org/10.1016/j.jcsr.2021.106872.
[37] G. Muciaccia, F. Giussani, G. Rosati, F. Mola, Response of self-compacting concrete filled tubes under eccentric compression, J. Constr. Steel Res 67 (5) (May 2011) 904–916, https://doi.org/10.1016/j.jcsr.2010.11.003.
[38] Z. Wang, et al., Buckling analysis of an innovative type of steel-concrete composite support in tunnels, J. Constr. Steel Res 179 (Apr. 2021) 106503, https://doi.org/10.1016/j.jcsr.2020.106503.
[39] ABAQUS, Explicit (2018) User's manual. Dassault Systemes Simulia Corporation, Paris".
[40] V. Karlos, G. Solomos, M. Larcher, Analysis of the blast wave decay coefficient using the Kingery–Bulmash data, Int. J. Prot. Struct. 7 (3) (Sep. 2016) 409–429, https://doi.org/10.1177/2041419616659572.
[41] J. Li, C. Wu, H. Hao, Y. Su, Z. Liu, Blast resistance of concrete slab reinforced with high performance fibre material, J. Struct. Integr. Maint. 1 (2) (Apr. 2016) 51–59, https://doi.org/10.1080/24705314.2016.1179496.